DOI: 10.1002/ejic.200800308

Binuclear Magnesium, Calcium and Zinc Complexes Based on Bis(salicylaldimine) Ligands with Rigid Bridges

Sven Range,[a] Dirk F.-J. Piesik,[a] and Sjoerd Harder*[a]

Keywords: Alkaline earth metals / Magnesium / Calcium / Zinc / Polylactide

Four dinucleating ligands based on sterically protected salicylaldimine units bridged by a variety of rigid groups have been prepared: 1,4-bis[(3,5-di-*tert*-butylsalicylidene)amino]-benzene (PARA-H_2), 1,3-bis[(3,5-di-*tert*-butylsalicylidene)-amino]benzene (META-H_2), 2,6-bis[(3,5-di-*tert*-butylsalicylidene)amino]pyridine (PYR-H_2) and 1,4-bis[(3,5-di-*tert*-butylsalicylidene)amino]-2,3,5,6-tetramethylbenzene (Me_4PARA-H_2). Reactions with $[(Me_3Si)_2N]_2Mg\cdot(thf)_2$ gave three new heteroleptic dinuclear magnesium complexes: PARA-$[MgN(SiMe_3)_2\cdot thf]_2$, META-$[MgN(SiMe_3)_2\cdot thf]_2$ and PYR-$[MgN(SiMe_3)_2\cdot thf]_2$. The complex PARA-$[MgN(SiMe_3)_2\cdot thf]_2$ was characterized by X-ray diffraction. Reactions with $[(Me_3Si)_2N]_2Ca\cdot(thf)_2$ gave mixtures of homoleptic and heteroleptic species. The homoleptic and heteroleptic calcium complexes [PARA-$Ca\cdot(thf)_2]_2$ and PARA-$[CaN(SiMe_3)_2\cdot(thf)_2]_2$ could be isolated and were structurally characterized. These complexes are not stable in solution. Attempted syntheses of Me_4PARA-$[CaN(SiMe_3)_2\cdot(thf)_2]_2$ gave insoluble coordination polymers of Me_4PARA-Ca. Reactions with $[(Me_3Si)_2N]_2Zn$ gave precipitates of homoleptic dinuclear zinc complexes of which PYR-Zn could be structurally characterized as a cyclic tetramer. The dinuclear magnesium complexes PARA-$[MgN(SiMe_3)_2\cdot thf]_2$, META-$[MgN(SiMe_3)_2\cdot thf]_2$ and PYR-$[MgN(SiMe_3)_2\cdot thf]_2$ are neither active in the polymerization of epoxides nor in the copolymerization of epoxide/CO_2 (cylohexene or propylene oxide) but initiate the polymerization of *rac*-lactide. Yields of isolated polylactide strongly depend on the bridging unit and the solvent.

Introduction

The use of well-defined alkaline-earth metal complexes in catalysis is rapidly growing.[1] This especially holds for applications in ring opening polymerization of polar monomers in which case the biocompatibility of the catalyst is of major importance.[2]

As increasing research efforts on multinuclear metal catalysts show that cooperative effects of neighbouring metal sites considerably influence activities and selectivities in catalytic transformations,[3] we became interested in binuclear alkaline-earth metal catalysts. The bimetallic nature of such a complex could not only drastically change its catalytic behaviour but also might allow conversions that are not possible with monometallic systems. For instance, reactions like the epoxide homopolymerization (or epoxide/CO_2 copolymerization) are highly dependent on the close proximity of two or more metals.[4] Metalloenzymes efficiently exploit such cooperative effects of metals at close range.[5]

In our current research we define the following goals: (a) syntheses of a range of dinucleating ligands based on sterically protected salicylaldimine units bridged by a variety of rigid groups (Scheme 1), (b) explore the feasibility to synthesize well-defined heteroleptic dinuclear alkaline-earth metal complexes that are stable against ligand exchange (Scheme 1), (c) investigate the use of these dinucleating ligands in the syntheses of closely related zinc complexes and (d) test heteroleptic dinuclear metal complexes in the catalytic polymerization of polar monomers.

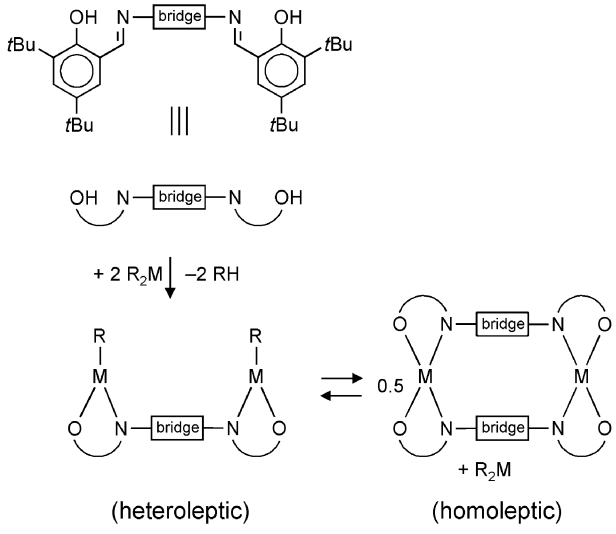

Scheme 1.

[a] Anorganische Chemie, Universität Duisburg-Essen, Universitätsstraße 5-7, 45117 Essen, Germany
E-mail: sjoerd.harder@uni-due.de

Results and Discussion

Ligand Choice and Syntheses

As ligands based on the N,O-chelating salicylaldimine unit are among the most easily accessible and tunable systems,[6] we concentrated on the syntheses of bis(salicylaldimine) complexes. Whereas flexible bridges allow fourfold chelation of the O,N,N,O-ligand, rigid bridges enable exclusive isolation of bimetallic complexes. Bulky *t*Bu substituents in the *o*-position are essential in order to prevent bridging of the phenolate oxygen atom and formation of coordination polymers. Four bis(salicylaldimine) ligands with rigid bridges were obtained in good yields (63–88%) by condensation of 3,5-di-*tert*-butylsalicylaldehyde with several diamines (Scheme 2). These ligands are abbreviated according to the nature of the bridge. The ligand with the rigid *p*-phenylene bridge (PARA-H_2, which has been used in the syntheses of dinuclear Al and Ga complexes)[7] and the permethylated *p*-phenylene bridge (Me_4PARA-H_2) fix the metal···metal distance in the range of circa 5.5–8.5 Å.[8] The ligand with the *m*-phenylene bridge (META-H_2, for which a dinuclear Zn complex is known)[9] is designed for bimetallic complexes in which the metal···metal distances can vary over a much larger range (circa 2.5–8 Å).[8] The ligand with the 2,5-pyridyl bridge (PYR-H_2) has been incorporated in these studies for potential coordination of the bridge's nitrogen atom to the metal(s).

Bis-magnesium Complexes

Bimetallic heteroleptic magnesium amide complexes have been prepared by twofold deprotonation of the bridged bis(salicylaldimine) ligands with two equivalents of $[(Me_3Si)_2N]_2Mg\cdot(thf)_2$ in benzene at room temperature. The complexes PARA-$[MgN(SiMe_3)_2\cdot(thf)]_2$, META-$[MgN(SiMe_3)_2\cdot$

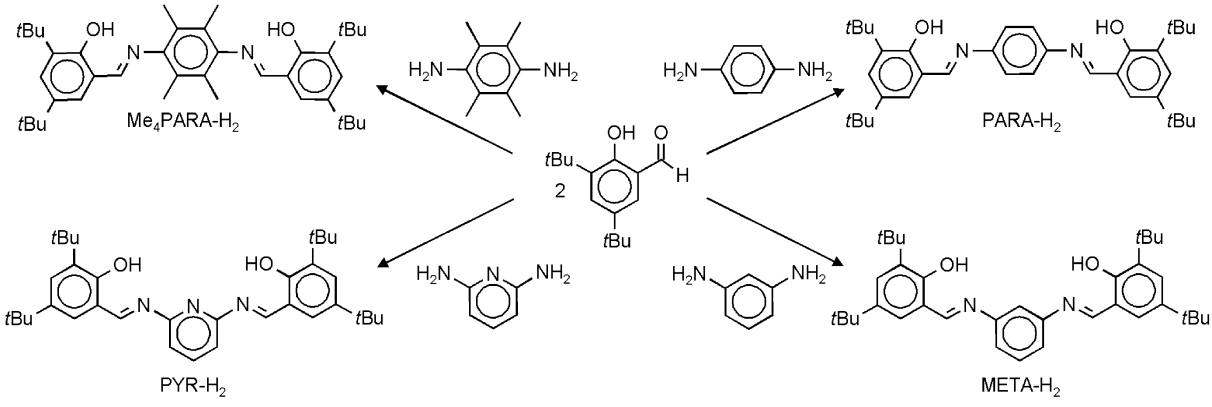

Scheme 2.

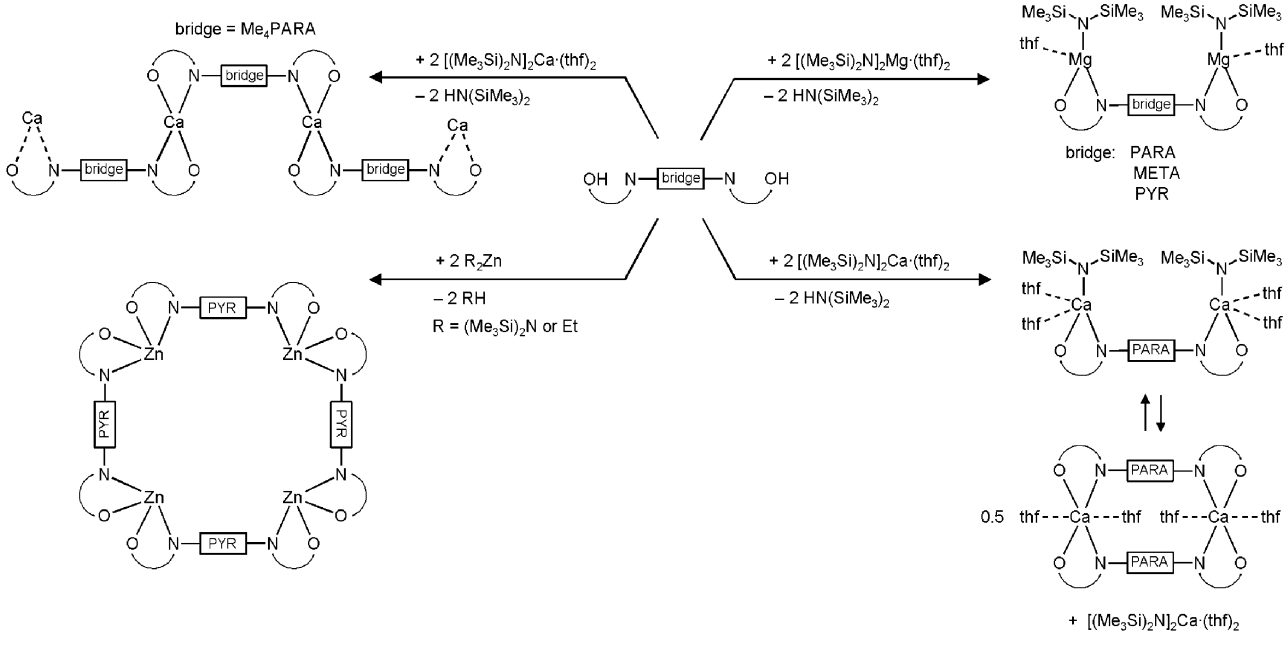

Scheme 3.

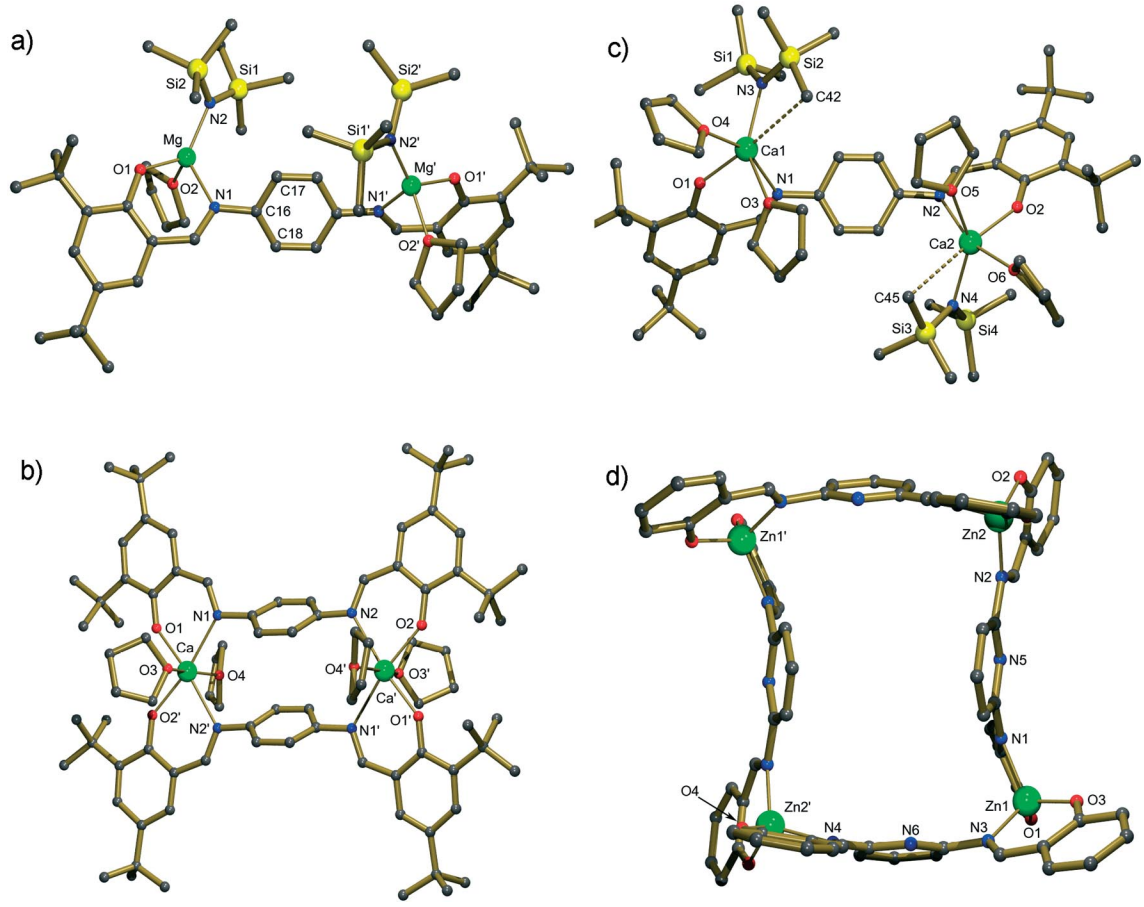

Figure 1. Crystal structures (hydrogen atoms omitted for clarity) of (a) PARA-[$MgN(SiMe_3)_2$·$(thf)]_2$, (b) [PARA-Ca·$(thf)_2]_2$, (c) PARA-[$CaN(SiMe_3)_2$·$(thf)_2]_2$ and (d) [PYR-Zn]$_4$ (*t*Bu substituents omitted for clarity; view along the crystallographic twofold rotation axis). Selected geometric parameters for all structures have been summarized in Table 1.

$(thf)]_2$ and PYR-[$MgN(SiMe_3)_2$·$(thf)]_2$ could be obtained crystalline pure in good yields (63–67%, Scheme 3).

The crystal structure of PARA-[$MgN(SiMe_3)_2$·$(thf)]_2$ (Figure 1a), described in detail below, shows two crystallographic identical (salicylaldimine)$MgN(SiMe_3)_2$·(thf) units connected by the *p*-phenylene bridge. The metal centers are situated at opposite sides of the bridge plane and show essentially no interaction [the Mg···Mg distance is 8.186(2) Å]. Crystals of META-[$MgN(SiMe_3)_2$·$(thf)]_2$ and PYR-[$MgN(SiMe_3)_2$·$(thf)]_2$ were too small for X-ray structure determination. Their compositions, however, indicate that the metal coordination geometries in these complexes are similar to that in PARA-[$MgN(SiMe_3)_2$·$(thf)]_2$.

In benzene or thf solutions all complexes are stable towards ligand exchange and the Schlenk equilibrium is, also at higher temperatures (60 °C), fully at the side of the heteroleptic species. The ^{1}H NMR spectra of PARA-[$MgN(SiMe_3)_2$·$(thf)]_2$, META-[$MgN(SiMe_3)_2$·$(thf)]_2$ and PYR-[$MgN(SiMe_3)_2$·$(thf)]_2$ consist of one set of signals for the bridging group and both salicylaldimine units as well as one singlet for the amide ligands. This implies essentially free rotation of the salicylaldimine units in respect to the bridge at room temperature.

Bis-Calcium Complexes

Deprotonation of the bridged salicylaldimine ligands with two equivalents of $[(Me_3Si)_2N]_2$Ca·$(thf)_2$ in benzene is fast, however, in all cases mixtures of homoleptic and heteroleptic complexes are observed (Scheme 3). This demonstrates the difficulties encountered in switching from magnesium to the considerably larger and softer calcium. Only in the case of the PARA ligand could we isolate a pure product: homoleptic [PARA-Ca·$(thf)_2]_2$ was obtained in the form of small yellow cube-like crystals. The crystal structure (Figure 1, b), which is discussed in detail below, shows a centrosymmetric dimeric complex. As the ^{1}H NMR spectrum of [PARA-Ca·$(thf)_2]_2$ dissolved in C_6D_6 displays numerous signals for the PARA-ligand, it should be concluded that in solution either several species exist or that a complicated aggregate with inequivalent ligand environments is formed (e.g. by dissociation of thf and reformation to higher aggregates).

Interestingly, when PARA-H_2 is deprotonated by two equivalents of $[(Me_3Si)_2N]_2$Ca·$(thf)_2$ in benzene, the initially formed small yellow cube-like crystals of [PARA-Ca·$(thf)_2]_2$ slowly disappear and several large yellow-orange

crystals with the shape of hexagons start to form (in one occasion the smaller crystals converted to just one new large hexagon). Single-crystal X-ray diffraction of these larger crystals revealed conversion of [PARA-Ca·(thf)$_2$]$_2$ into the heteroleptic complex PARA-[CaN(SiMe$_3$)$_2$·(thf)$_2$]$_2$. The crystal structure, described below in detail, shows a C_2-symmetric monomer (Figure 1, c). As can be seen by ^{1}H NMR analysis on crystalline pure samples of PARA-[CaN(SiMe$_3$)$_2$·(thf)$_2$]$_2$ dissolved in C_6D_6, in solution PARA-[CaN(SiMe$_3$)$_2$·(thf)$_2$]$_2$ converts back to [(Me$_3$Si)$_2$N]$_2$Ca·(thf)$_2$ and several homoleptic PARA-Ca·(thf)$_x$ species over a time period of several hours. In solution, this Schlenk equilibrium can be completely shifted back again to the heteroleptic species, PARA-[CaN(SiMe$_3$)$_2$·(thf)$_2$]$_2$, by addition of circa two equivalents of [(Me$_3$Si)$_2$N]$_2$Ca·(thf)$_2$. The equilibria between solid state and solution structures are represented in Scheme 4.

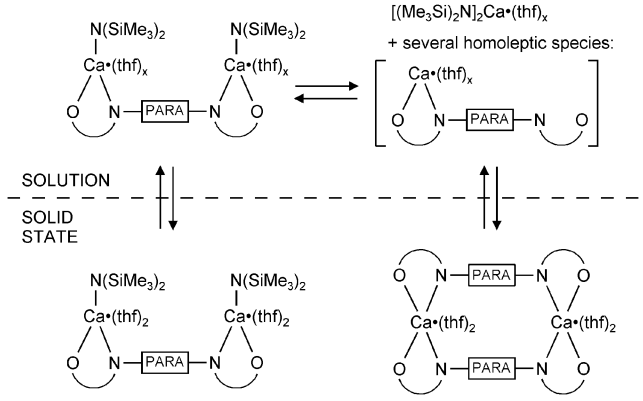

Scheme 4.

Although the compounds [PARA-Ca·(thf)$_2$]$_2$ and PARA-[CaN(SiMe$_3$)$_2$·(thf)$_2$]$_2$ are not stable in solution, solid-state structures could be obtained in both cases. Especially noteworthy is complete conversion of the small crystals (cube-like) of the homoleptic complex [PARA-Ca·(thf)$_2$]$_2$ into very large crystals (hexagons) of the heteroleptic complex PARA-[CaN(SiMe$_3$)$_2$·(thf)$_2$]$_2$. Although homoleptic species are favoured in solution, the heteroleptic complex is favoured in the solid state. This is likely due to the size of the crystals. According to the Gibbs–Thomson rule small crystals dissolve more readily than larger ones whereas large crystals grow faster; i.e. under reversible crystallization/dissolution conditions larger crystals grow at cost of smaller ones. According to this principle, which is called Ostwald ripening,[10] the larger crystals of the heteroleptic complex PARA-[CaN(SiMe$_3$)$_2$·(thf)$_2$]$_2$ are favoured. Although Ostwald ripening has been successfully applied in enantiomer trapping,[11] this is the first example of converting a crystalline homoleptic calcium complex into a crystalline heteroleptic complex that is unstable in solution.

Detailed analysis (vide infra) of the crystal structure of [PARA-Ca·(thf)$_2$]$_2$ shows that the phenylene bridges attract each other (Figure 2). This favourable π-π stacking interaction might be the driving force for formation of homoleptic complexes in solution. We reasoned that use of a permethylated phenylene bridge (like in Me$_4$PARA) could avoid formation of the homoleptic dimer and might be the key to a stable heteroleptic bis-calcium complex Me$_4$PARA-[CaN(SiMe$_3$)$_2$·(thf)$_2$]$_2$. Reaction of Me$_4$PARA-H$_2$ with two equivalents of [(Me$_3$Si)$_2$N]$_2$Ca·(thf)$_2$ gave a precipitate that is completely insoluble in benzene as well as in thf. ^{1}H NMR analysis of the solid quenched in CD$_3$OD revealed a homoleptic product that only contains the Me$_4$PARA-ligand. We propose a polymeric structure in which Ca^{2+} ions bridge between different ligands (Scheme 3).

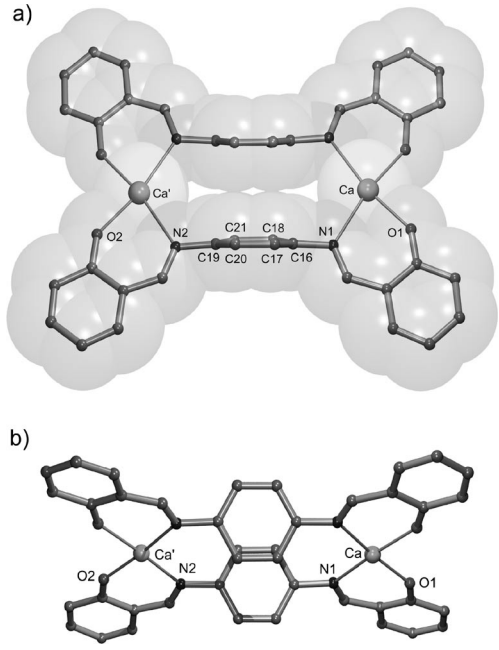

Figure 2. Partial structure of [PARA-Ca·(thf)$_2$]$_2$. (a) The view along the bridge planes shows the attractive interaction between the phenylene bridges. (b) The view perpendicular on the bridge plane shows the off-set stacking of the π-π interaction.

Bis-Zinc Complexes

Reaction of the bis(salicylaldimide) ligand PARA-H$_2$ with two equivalents of Et$_2$Zn in benzene at room temperature resulted in the expected evolution of ethane but gave a complex mixture of species from which no distinct product could be isolated. Reactions of the ligands META-H$_2$ or PYR-H$_2$ with two equivalents of Et$_2$Zn gave exclusive precipitation of the homoleptic complexes META-Zn (which has been described before)[9] and PYR-Zn. Even with a large excess of Et$_2$Zn (> 10 equiv.) only homoleptic complexes could be isolated. Also addition of Lewis bases like thf did not enable isolation of heteroleptic species. Likewise, reactions of the ligands with [(Me$_3$Si)$_2$N]$_2$Zn gave exclusively homoleptic complexes. For one of the homoleptic products we have been able to isolate single crystals suitable for X-ray diffraction. The crystal structure of (PYR)Zn (Figure 1, d), which is described in detail below, shows a tetrameric aggregrate: [(PYR)Zn]$_4$. Selforganization to this supramolecular quadrangle can be rationalized by the fact

that two mutual perpendicular N,O-chelating salicylaldimine units coordinate at a common Zn center in tetrahedral fashion, thus creating 90° angles between these ligands. Such selforganization to intriguing metallosupramolecular structures is quite common for salicylaldimine zinc complexes.[12]

Crystal Structures

PARA-[MgN(SiMe$_3$)$_2$·(thf)]$_2$ crystallizes as a crystallographically C_2-symmetric complex [Figure 1 (a), Table 1]. Each Mg^{2+} ion binds to a N,O-chelating salicylaldimine unit, a $(Me_3Si)_2N^-$ ion and a THF ligand. The coordination geometry of Mg^{2+} can be described as a distorted tetrahedron. The Mg–O/Mg–N bond lengths and the N,O-bite angle of the salicylaldimine unit [90.4(1)°] are comparable to those in another salicylaldimine magnesium complex.[13] The dihedral angle between the salicylaldimine plane and the phenylene bridge is 35.2(1)°. A coplanar arrangement of the salicylaldimine unit and the phenylene bridge is unfavourable on account of repulsion between the N=CH hydrogen atom and a hydrogen atom in the phenylene bridge. This repulsive interaction is not only underscored by short H···H distances but also by the acute C17–C16–N1 angle of 117.4(3)° and the obtuse C18–C16–N1 angle of 124.5(3)°. No obvious agostic Mg···H interactions are observed. This non-planar arrangement of salicylaldimine units and the imine substituents is commonly observed in metal complexes with chelating salicylaldimine ligands and is related to the bland yellowish colour of these compounds: planar arrangements give rise to delocalization and stronger colours (usually orange-red like in the protonated ligands).[13]

Table 1. Selected bond lengths [Å] and angles [°] for the crystal structures of PARA-[MgN(SiMe$_3$)$_2$·(thf)]$_2$, [PARA-Ca·(thf)$_2$]$_2$, PARA-[CaN(SiMe$_3$)$_2$·(thf)$_2$]$_2$ and [PYR-Zn]$_4$.

PARA-[MgN(SiMe$_3$)$_2$·(thf)]$_2$					
Mg–O1	1.914(3)	N1–Mg–O1	90.4(1)	N1–Mg–O2	98.2(1)
Mg–N1	2.097(3)	N1–Mg–N2	122.1(2)	O1–Mg–O2	98.7(1)
Mg–O2	2.032(3)	O2–Mg–N2	117.3(1)	O1–Mg–N2	123.9(1)
Mg–N2	1.980(3)				
[PARA-Ca·(thf)$_2$]$_2$					
Ca–N1	2.520(5)	N1–Ca–O1	74.7(2)	O1–Ca–O2′	96.8(2)
Ca–O1	2.215(4)	N2′–Ca–O2′	74.5(2)	N1–Ca–N2′	114.4(2)
Ca–O3	2.362(4)	O3–Ca–O4	164.7(2)	O1–Ca–O3	97.1(1)
Ca–O4	2.382(4)	O1–Ca–O4	92.2(2)		
PARA-[CaN(SiMe$_3$)$_2$·(thf)$_2$]$_2$					
Ca1–O1	2.179(4)	N1–Ca1–O1	74.8(2)	O1–Ca1–O4	90.5(2)
Ca1–N1	2.459(6)	N1–Ca1–O3	85.1(2)	O1–Ca1–N3	121.3(2)
Ca1–O3	2.413(5)	N1–Ca1–O4	161.3(2)	O3–Ca1–O4	85.1(2)
Ca1–N3	2.328(5)	N1–Ca1–N3	101.2(2)	O3–Ca1–N3	142.4(2)
Ca1–O4	2.401(5)	O1–Ca1–O3	96.2(2)	O4–Ca1–N3	96.3(2)
Ca2–O2	2.157(4)	N2–Ca2–O2	75.2(2)	O2–Ca2–O6	89.6(2)
Ca2–N2	2.507(6)	N2–Ca2–O5	81.0(2)	O2–Ca2–N4	122.2(2)
Ca2–N4	2.292(5)	N2–Ca2–O6	156.7(2)	O5–Ca2–O6	83.7(2)
Ca2–O5	2.398(5)	N2–Ca2–N4	105.2(2)	O5–Ca2–N4	139.8(2)
Ca2–O6	2.383(6)	O2–Ca2–O5	97.9(2)	O6–Ca2–N4	97.8(2)
[PYR-Zn]$_4$					
Zn1–O1	1.904(2)	O1–Zn1–N1	96.9(1)	N1–Zn1–O3	114.6(1)
Zn1–N1	1.999(3)	O1–Zn1–O3	122.5(1)	N1–Zn1–N3	111.8(1)
Zn1–O3	1.895(2)	O1–Zn1–N3	116.5(1)	O3–Zn1–N3	95.5(1)
Zn1–N3	1.990(3)				
Zn2–O2	1.913(2)	O2–Zn2–N2	96.6(1)	N2–Zn2–O4′	116.3(1)
Zn2–N2	1.991(3)	O2–Zn2–O4′	120.8(1)	N2–Zn2–N4′	114.0(1)
Zn2–O4′	1.919(4)	O2–Zn2–N4′	115.6(1)	O4′–Zn2–N4′	95.0(1)
Zn2–N4′	2.026(3)				

[PARA-Ca·(thf)$_2$]$_2$ crystallizes as a crystallographic centrosymmetric dimer [Figure 1 (b), Table 1]. Each Ca^{2+} ion binds to two N,O-chelating salicylaldimine units and two THF ligands. The distance between the two Ca^{2+} ions measures 8.380(2) Å. The salicylaldimine ligands at a common metal center are nearly coplanar [dihedral angle N1–Ca–O1/N2′–Ca–O2′ 7.3(2)°]. The N,O-bite angle of the salicylaldimine unit (average: 74.6°) is considerably smaller than that in the Mg complex PARA-[MgN(SiMe$_3$)$_2$·(thf)]$_2$. Therefore, the coordination geometry for Ca^{2+} is slightly distorted from octahedral. The oxygen atoms of the THF ligands bend somewhat inwards [O3–Ca–O4 164.7(2)°] on account of the bulky *t*Bu substituents in the periphery. The salicylaldimine units make angles of 57.3(2)° and 63.2(2)° with the phenylene bridge thus partially shutting off delocalization in the PARA ligand system. As these dihedral angles are larger than those in PARA-[MgN(SiMe$_3$)$_2$·(thf)]$_2$, repulsion between the N=CH hydrogen atom and the bridge is relaxed. The phenylene bridge itself is considerably deviated from planarity as can be seen from a view parallel to the bridge (Figure 2, a). The carbon atoms C17, C18, C20 and C21 are arranged in a plane (maximum deviation from a least-squares plane is 0.006 Å) but carbon atoms C16 and C19 are situated 0.691(6) Å and 0.694(6) Å, respectively, out of this plane. This attraction between the bridges can be explained by a strong π-π stacking interaction.[14] The ring–ring distance of 3.412(8) Å is indeed similar to that of the layer distance in graphite (3.40 Å). The view perpendicular on the bridge planes shows that the rings are slipped in respect to each other [Figure 2 (b); ring slippage 2.117 Å]. This off-set stacking interaction allows for an optimal mutual attraction between $C^{\delta-}$–$H^{\delta+}$ dipoles of one phenylene unit and the π-system of the other bridge.

PARA-[CaN(SiMe$_3$)$_2$·(thf)$_2$]$_2$ crystallizes as a monomer with approximate C_2-symmetry [Figure 1 (c), Table 1]. The Ca–N(SiMe$_3$)$_2$ units are situated on the same side of the phenylene bridge with a Ca···Ca distance of 8.251(2) Å. Each Ca^{2+} ion is bound to one N, O-chelating salicylaldimine unit, one $(Me_3Si)_2N^-$ ion and two THF ligands. The calcium coordination geometries can be described as distorted trigonal bipyramidal. For Ca1 axial positions are envisioned for N1 and O4 and for Ca2 the atoms N2 and O6 occupy the axial positions. For each Ca^{2+} ion one rather large N–Ca–O angle is observed in the equatorial plane [N3–Ca1–O3 142.4(2)° and N4–Ca2–O5 139.8(2)°]. This is due to an agostic interaction between a Me_3Si substituent and Ca^{2+} as is evident from Ca···C distances considerably shorter than the sum of the van der Waals radii of Ca and C (3.49 Å): the Ca1···C42 and Ca2···C45 distances are 3.153(8) Å and 3.191(8) Å, respectively. These agostic

Me···Ca interactions also cause significant tilting of the amide ligand with respect to the Ca–N axes: one of the Ca–N–Si angles is widened [Ca1–N3–Si1 121.9(3)° and Ca2–N4–Si4 121.8(3)°] whereas the other is squeezed [Ca1–N3–Si2 109.8(3)° and Ca2–N4–Si3 112.3(3)°].

[PYR-Zn]$_4$ crystallizes as a crystallographically C_2-symmetric cyclic tetrameric aggregate [Figure 1 (d), Table 1]. Both crystallographically unique Zn metals (Zn1 and Zn2) are chelated by two nearly perpendicularly oriented salicylaldimine units [dihedral angles: N1–O1–Zn1/N3–O3–Zn1 89.2(1)° and N2–O2–Zn2/N4′–O4′–Zn2 89.0(1)°]. In comparison to the other structures described in this paper, the bis(salicylaldimine) ligands in [PYR-Zn]$_4$ display a more pronounced planarity. The dihedral angles between salicylaldimine and pyridyl planes are 8.0(1)°, 14.4(1)°, 31.9(1)° and 37.6(1)°. Whereas the conformations of the PARA and META ligands are partially determined by repulsion between the N=CH hydrogen atom and the bridge, the PYR ligand in [PYR-Zn]$_4$ avoids such repulsive interaction by the *cisoid* arrangement of N=CH hydrogen and pyridyl nitrogen atoms. Instead, attractive non-classical C–H···N hydrogen bridges are observed: the H···N distances range from 2.15–2.46 Å and are well below the sum of their van der Waals radii (2.75 Å; C–H···N angles range from 101–108°). The Zn–O and Zn–N bond lengths are within the range observed for other salicylaldimine zinc complexes.[15]

Polymerization Studies

At room temperature the heteroleptic bimetallic complexes PARA-[MgN(SiMe$_3$)$_2$·(thf)]$_2$, META-[MgN(SiMe$_3$)$_2$·(thf)]$_2$ and PYR-[MgN(SiMe$_3$)$_2$·(thf)]$_2$ do not react with cyclohexene oxide or propylene oxide. Increasing the reaction temperature to 60 °C gave protonation of the amide $(Me_3Si)_2N^-$. Although no products could be isolated from this reaction, we presume that the amide base deprotonated the epoxide to form an enolate. Similar enolate formation has been unequivocally proven in reaction of **1** with cyclohexene oxide.[2d] Like the monometallic complex **1**, also the bimetallic magnesium catalysts are not active in the homopolymerization of cyclohexene and propylene oxide. As recently a bimetallic magnesium catalyst (**2**) has been introduced for the epoxide/CO_2 copolymerization,[16] our bimetallic magnesium amides were also tested in the copolymerization of neat cyclohexene oxide with CO_2 (10 bar). Under various conditions no activity for copolymerization could be observed.

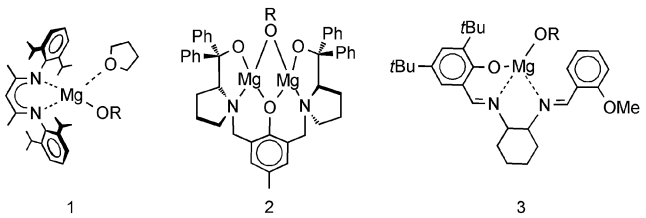

1 2 3

All heteroleptic bimetallic complexes PARA-[MgN(SiMe$_3$)$_2$·(thf)]$_2$, META-[MgN(SiMe$_3$)$_2$·(thf)]$_2$ and PYR-[MgN(SiMe$_3$)$_2$·(thf)]$_2$ are active in the polymerization of *rac*-lactide (*rac*-LA). Although magnesium complexes are generally among the most active catalysts for lactide polymerization,[2c,2d] the bimetallic magnesium catalysts are only moderately active. Whereas the β-diketiminate catalyst **1** reaches full conversion of monomer after one minute,[2c] PARA-[MgN(SiMe$_3$)$_2$·(thf)]$_2$ gave under similar conditions 70% conversion after 60 min (as determined by ^{1}H NMR). It is, however, comparable in activity with a recent mononuclear salicylaldimine magnesium catalyst **3**, for which under similar conditions 59% conversion was observed after one hour.[2i] The results of a series of polymerization experiments with three different catalysts in three different solvents (thf, CH_2Cl_2 and toluene) and work-up after five hours have been summarized in Table 2.

Table 2. Polymerization of *rac*-LA using the heteroleptic magnesium complexes PARA-[MgN(SiMe$_3$)$_2$·thf]$_2$, META-[MgN(SiMe$_3$)$_2$·thf]$_2$ and PYR-[MgN(SiMe$_3$)$_2$·thf]$_2$; ratio [LA]:[Mg] = 50:1 (expected $M_n = 7.2 \times 10^3$ Da); polymerization time = 5 h.

Catalyst	T [°C]	Solvent	Yield (%)	$M_n \times 10^3$	PDI
PARA-[MgN(SiMe$_3$)$_2$·thf]$_2$	20	thf	79	18.3	1.97
META-[MgN(SiMe$_3$)$_2$·thf]$_2$	20	thf	56	18.7	1.76
PYR-[MgN(SiMe$_3$)$_2$·thf]$_2$	20	thf	35	17.5	1.62
PARA-[MgN(SiMe$_3$)$_2$·thf]$_2$	20	CH_2Cl_2	43	19.9	1.79
META-[MgN(SiMe$_3$)$_2$·thf]$_2$	20	CH_2Cl_2	22	17.6	1.67
PYR-[MgN(SiMe$_3$)$_2$·thf]$_2$	20	CH_2Cl_2	81	16.6	1.44
PARA-[MgN(SiMe$_3$)$_2$·thf]$_2$	80[a]	toluene	36	14.6	1.42
META-[MgN(SiMe$_3$)$_2$·thf]$_2$	80[a]	toluene	30	13.4	1.45
PYR-[MgN(SiMe$_3$)$_2$·thf]$_2$	80[a]	toluene	72	17.1	1.66

[a] Due to the poor solubility of *rac*-LA in toluene the temperature has been raised to 80 °C.

Isolated yields strongly depend on the solvent used and the nature of the bridging unit (Table 2). The *p*-phenylene-bridged catalysts generally give higher polylactide yields than the *m*-phenylene-bridged ones. Whereas the pyridyl-bridged catalyst is not very active in thf, it is superior to the phenylene-bridged systems in less polar solvents like CH_2Cl_2 and toluene. This indicates that in an apolar medium the intramolecular coordination of the pyridyl nitrogen at the metal center might play a role in the polymerization mechanism.

The molecular weights of the polymers obtained are in all cases considerably higher than the molecular weight expected based on the Mg/lactide ratio of 1:50 (7200 Da). This indicates either that propagation is faster than initiation or that partial hydrolysis of the initiating functionality has occurred. As it has been observed before that the $(Me_3Si)_2N$ ligand is slow in initiating lactide polymerization,[2c,2d] slow initiation is the most likely explanation. Whereas the salicylaldimine magnesium catalyst **3** gave polylactides with very narrow molecular weight distributions (PDI: 1.05–1.10), the bimetallic magnesium catalysts gave less controlled polymerization (PDI: 1.42–1.97). We tentatively attribute the broad molecular weight distributions to slow initiation as well as transesterification processes (backbiting).

Although the tacticities of the obtained polymers vary slightly with the nature of the bridge and the solvent used, all polymers should be regarded as mainly atactic. This con-

trasts with the mononuclear magnesium catalyst **1** which in a polar medium (thf) gives heterotactic polylactide.[2d]

Conclusions

Heteroleptic bimetallic magnesium amide complexes with a variety of bridged bis(salicylaldimine) ligands have been obtained. These complexes are also stable in solution (C_6D_6 as well [D_8]THF) even under forced reflux conditions. Switching to the heavier congener Ca led to dynamic mixtures of homoleptic and heteroleptic complexes. However, homoleptic as well as heteroleptic calcium complexes could be obtained in the solid state. Interestingly, crystals of the homoleptic complex convert to crystals of the heteroleptic complex on account of Ostwald ripening. Stable heteroleptic bimetallic zinc amide complexes cannot be obtained with the bis(salicylaldimine) ligands used in this study. Instead, spontaneous self-organization to large supramolecular multimetallic zinc aggregates is observed.

Although the heteroleptic bimetallic magnesium amides were not effective in the homopolymerization of epoxides or in the copolymerization of CO_2 and epoxides, polylactide could be obtained in a variety of solvents. The isolated yield of polymer is strongly dependent on the nature of the bridging unit and the solvent used. Whereas the phenylene-bridged catalysts are more effective under polar conditions, the pyridyl-bridged catalyst shows higher activity in apolar solvents. This indicates that the intramolecular coordination of the pyridyl nitrogen at the metal center might play a role in the polymerization mechanism.

Experimental Section

General Remarks: All manipulations were performed under a dry and oxygen-free atmosphere (argon or nitrogen) using Schlenk line and glove box techniques and freshly dried solvents. Following complexes have been prepared according to literature: 3,5-di-*tert*-butylsalicylaldehyde,[17] $[(Me_3Si)_2N]_2Mg\cdot(thf)_2$,[18] $[(Me_3Si)_2N]_2Ca\cdot(thf)_2$ [18] and $(Me_3SiN)_2Zn$.[19]

General Synthesis of Bridged Bis(salicylaldimine) Ligands (see Scheme 1): A stirred solution of 3,5-di-*tert*-butylsalicylaldehyde (3.75 g, 16.0 mmol) and 8.0 mmol of the selected diamine in methanol (150 mL) was heated at reflux temperature for 2 h. The reaction mixture was cooled to room temperature and stirred overnight. The coloured precipitate was filtered and washed with methanol (5 × 80 mL). The resulting solid was dissolved in thf (120 mL) and dried with molecular sieves for 6 h at reflux temperature. After separation of the molecular sieves the solvent was removed under reduced pressure to give a coloured solid.

PARA-H_2: Orange solid (yield: 3.81 g, 88%); m.p. 307 °C. ^{1}H NMR (300 MHz, C_6D_6, 25 °C): δ = 14.2 (s, 2 H, O*H*), 8.13 (s, 2 H, C*H*N), 7.67 [d, ^4J(H,H) = 2.3 Hz, 2 H, H_{aryl}], 7.08 [d, ^4J(H,H) = 2.3 Hz, 2 H, H_{aryl}], 6.89 (s, 4 H, H_{aryl}), 1.71 (18 H, *t*Bu), 1.37 (s, 18 H, *t*Bu) ppm. ^{13}C NMR (300 MHz, C_6D_6, 25 °C): δ = 163.5, 159.1, 147.1, 140.7, 137.5, 128.2, 127.4, 122.4, 119.0, 35.5, 34.3, 31.7, 29.8 ppm. $C_{36}H_{48}N_2O_2$ (540.80): calcd. C 79.96, H 8.95; found C 80.15, H 8.81.

META-H_2: Orange solid (yield: 3.55 g, 82%); m.p. 187 °C. ^{1}H NMR (300 MHz, C_6D_6, 25 °C): δ = 14.1 (s, 2 H, O*H*), 8.13 (s, 2 H, C*H*N), 7.67 [d, ^4J(H,H) = 2.3 Hz, 2 H, H_{aryl}], 7.09 [d, ^4J(H,H) = 2.4 Hz, 2 H, H_{aryl}], 7.04 [t, ^4J(H,H) = 8.1 Hz, 1 H, H_{aryl}], 6.82–6.77 (m, 3 H, H_{aryl}) 1.71 (s, 18 H, *t*Bu), 1.36 (s, 18 H, *t*Bu) ppm. ^{13}C NMR (300 MHz, C_6D_6, 25 °C): δ = 164.6, 159.2, 149.9, 140.7, 137.5, 130.1, 127.5, 119.7, 118.9, 114.2, 35.5, 34.3, 31.7, 29.7 ppm. $C_{36}H_{48}N_2O_2$ (540.80): calcd. C 79.96, H 8.95; found C 80.27, H 8.98.

PYR-H_2: Orange solid (yield: 2.73 g, 63%); m.p. 237 °C. ^{1}H NMR (300 MHz, C_6D_6, 25 °C): δ = 14.5 (s, 2 H, O*H*), 9.43 (s, 2 H, C*H*N), 7.64 [d, ^4J(H,H) = 2.3 Hz, 2 H, H_{aryl}], 7.12 [d, ^4J(H,H) = 2.3 Hz, 2 H, H_{aryl}], 7.04 [t, ^3J(H,H) = 7.6 Hz, 1 H, H_{aryl}], 6.72 [d, ^3J(H,H) = 7.7 Hz, 2 H, H_{Aryl}], 1.69 (s, 18 H, *t*Bu), 1.21 (s, 18 H, *t*Bu) ppm. ^{13}C NMR (300 MHz, C_6D_6, 25 °C): δ = 166.2, 160.1, 140.9, 140.3, 137.5, 129.1, 128.6, 119.0, 118.7, 35.5, 34.2, 31.5, 29.7 ppm. $C_{35}H_{47}N_3O_2$ (541.78): calcd. C 77.59, H 8.74; found C 77.72, H 8.51.

Me_4PARA-H_2: Pale yellow solid (yield: 3.34 g, 70%); m.p. 298 °C. ^{1}H NMR (300 MHz, C_6D_6, 25 °C): δ = 14.1 (s, 2 H, O*H*), 7.88 (s, 2 H, C*H*N), 7.67 [d, ^4J(H,H) = 2.0 Hz, 2 H, H_{aryl}], 7.10 [d, ^4J(H,H) = 2.1 Hz, 2 H, H_{aryl}], 1.96 (s, 12 H, CH_3), 1.69 (s, 18 H, *t*Bu), 1.34 (s, 18 H, *t*Bu) ppm. ^{13}C NMR (300 MHz, C_6D_6, 25 °C): δ = 168.8, 159.2, 146.4, 137.7, 128.1, 127.1, 125.2, 118.7, 35.5, 34.3, 31.6, 29.8, 15.3 ppm. $C_{40}H_{56}N_2O_2$ (596.90): calcd. C 80.49, H 9.46; found C 80.61, H 9.32.

PARA-$[MgN(SiMe_3)_2\cdot thf]_2$: To a stirred solution of $[(Me_3Si)_2N]_2Mg\cdot(thf)_2$ (1.96 g, 4.01 mmol) in benzene (5.0 mL) was added PARA-H_2 (1.00 g, 1.85 mmol). The yellow solution was stirred for 16 h at room temperature. The solution was concentrated to slightly less than half of its original volume. After slowly cooling to 5 °C yellow crystals of PARA-$[MgN(SiMe_3)_2\cdot thf]_2$ precipitated: 1.28 g (66%); m.p. 231 °C. ^{1}H NMR (300 MHz, C_6D_6, 25 °C): δ = 8.21 (s, 2 H, NC*H*), 7.77 [d, ^4J(H,H) = 2.6 Hz, 2 H, H_{aryl}], 7.48 (s, 4 H, H_{aryl}), 7.09 [d, ^4J(H,H) = 2.6 Hz, 2 H, H_{aryl}], 3.50 (m, THF), 1.74 (s, 18 H, *t*Bu), 1.35 (s, 18 H, *t*Bu), 1.09 (m, THF), 0.40 (s, 36 H, Me_3Si) ppm. ^{13}C NMR (300 MHz, C_6D_6, 25 °C): δ = 171.7, 169.3, 149.5, 141.7, 135.9, 131.6, 130.8, 123.7, 120.2, 69.3, 35.8, 34.1, 31.6, 30.0, 24.9, 6.13 ppm. $C_{56}H_{98}Mg_2N_4O_4Si_4$ (1052.38): calcd. C 63.91, H 9.39; found C 63.74, H 9.21.

META-$[MgN(SiMe_3)_2\cdot thf]_2$: To a stirred solution of $[(Me_3Si)_2N]_2Mg\cdot(thf)_2$ (1.90 g, 3.89 mmol) in benzene (5.0 mL) was added META-H_2 (1.00 g, 1.85 mmol). The yellow solution was stirred for 16 h at room temperature. All solvents were removed under reduced pressure and the yellow solid was dissolved in hexane. After cooling slowly cooling the hexane solution –28 °C small yellow crystals precipitated. The crystalline product was isolated, washed three times with cold hexane and dried at 40 °C under high vacuum: 1.22 g (63%); m.p. 231 °C. ^{1}H NMR (300 MHz, C_6D_6, 25 °C): δ = 8.36 (s, 2 H, NC*H*), 7.77 [d, ^4J(H,H) = 2.3 Hz, 2 H, H_{aryl}], 7.43 (s, 1 H, H_{aryl}), 7.33 (s, 3 H, H_{aryl}), 7.20 [d, ^4J(H,H) = 2.3 Hz, 2 H, H_{aryl}], 3.54 (m, THF), 1.73 (s, 18 H, *t*Bu), 1.36 (s, 18 H, *t*Bu), 1.08 (m, THF), 0.39 (s, 36 H, Me_3Si) ppm. ^{13}C NMR (300 MHz, C_6D_6, 25 °C): δ = 172.4, 169.4, 152.9, 141.7, 136.0, 131.8, 131.0, 121.3, 120.1, 114.3, 69.6, 35.8, 34.1, 31.6, 29.9, 24.8, 6.54 ppm. $C_{56}H_{98}Mg_2N_4O_4Si_4$ (1052.38): calcd. C 63.91, H 9.39; found C 63.66, H 9.28.

PYR-$[MgN(SiMe_3)_2\cdot thf]_2$: To a stirred solution of $[(Me_3Si)_2N]_2Mg\cdot(thf)_2$ (1.96 g, 4.01 mmol) in benzene (5.0 mL) was added PYR-H_2 (1.00 g, 1.85 mmol). The orange solution was stirred for 16 h at room temperature. All solvents were removed under reduced pressure and the orange solid was dissolved in hexane. Slowly cooling

the hexane solution to –80 °C gave a precipitate of fine orange needle-like crystals which were isolated and washed three times with cold hexane. The product was dried at 40 °C under high vacuum: 1.31 g (67%); m.p. 138 °C. ^{1}H NMR (300 MHz, C_6D_6, 25 °C): δ = 9.18 (s, 2 H, NC*H*), 7.78 [d, ^4J(H,H) = 2.6 Hz, 2 H, H_{aryl}], 7.52–7.46 (m, 3 H, H_{aryl}), 7.23 [d, ^4J(H,H) = 2.6 Hz, 2 H, H_{aryl}], 3.58 (m, THF), 1.72 (s, 18 H, *t*Bu), 1.36 (s, 18 H, *t*Bu), 1.04 (m, THF), 0.41 (s, 36 H, Me_3Si) ppm. ^{13}C NMR (300 MHz, C_6D_6, 25 °C): δ = 171.0, 159.7, 142.2, 140.1, 136.2, 132.7, 131.5, 127.9, 119.7, 115.8, 69.2, 35.8, 34.1, 31.5, 29.0, 25.0, 6.18 ppm. $C_{55}H_{97}Mg_2N_5O_4Si_4$ (1053.37): calcd. C 62.71, H 9.28; found C 62.55, H 9.12.

[PARA-Ca·(thf)$_2$]$_2$: To a stirred solution of $[(Me_3Si)_2N]_2Ca\cdot(thf)_2$ (1.96 g, 3.88 mmol) in benzene (12.0 mL) was added PARA-H_2 (1.00 g, 1.85 mmol). The yellow solution was stirred for 5 h at room temperature. Slow cooling to +5 °C gave overnight small yellow cube-like crystals which were isolated, washed twice with cold benzene and dried under high vacuum: 1.98 g (74%); m.p. 238 °C (dec.). The crystals dissolve poorly in C_6D_6 and [D$_8$]THF and in both cases numerous sets of signals are observed in the ^{1}H NMR spectra. It is likely that in solution either several species exist or that a complicated aggregate with inequivalent ligand environments is formed. $C_{88}H_{124}Ca_2N_4O_8$ (1446.15): calcd. C 73.09, H 8.64; found C 72.73, H 8.67.

PARA-[CaN(SiMe$_3$)$_2$·(thf)$_2$]$_2$: To a stirred solution of $[(Me_3Si)_2N]_2Ca\cdot(thf)_2$ (1.02 g, 2.02 mmol) in benzene (8.0 mL) was added PARA-H_2 (0.50 g, 0.93 mmol). The yellow solution was stirred for 5 h at room temperature. Slow cooling to +5 °C gave overnight small yellow cube-like crystals (0.1 × 0.1 × 0.1 mm) which after standing for 3 d at +5 °C completely dissolved again and new rather large yellow/orange crystals (4 × 4 × 0.5 mm) in the form of a hexagon precipitated. The new crystals were isolated, washed twice with cold benzene and dried under high vacuum: 0.50 g (44%); m.p. 172 °C. ^{1}H NMR (300 MHz, C_6D_6, 25 °C): δ = 8.37 (s, 2 H, NC*H*), 7.72 (d, ^4J(H,H) = 2.5 Hz, 2 H, H_{aryl}), 7.62 (s, 4 H, H_{aryl}), 7.23 [d, ^4J(H,H) = 2.5 Hz, 2 H, H_{aryl}], 3.64 (m, 16 H, THF), 1.75 (s, 18 H, *t*Bu), 1.30 (s, 18 H, *t*Bu), 0.34 (s, 36 H, Me_3Si) ppm. ^{13}C NMR (300 MHz, C_6D_6, 25 °C): δ = 170.4, 168.7, 151.9, 140.2, 133.9, 131.4, 130.0, 128.3, 123.5, 122.1, 69.5, 35.8, 34.0, 31.8, 30.0, 25.1, 5.92 ppm. $C_{64}H_{114}Ca_2N_4O_6Si_4$ (1228.15): calcd. C 62.59, H 9.36; found C 62.18, H 9.16.

[PYR-Zn]$_4$: To a stirred solution of PYR-H_2 (1.00 g, 1.85 mmol) in benzene (8.0 mL) was added Et_2Zn (1.85 mL of a 1 M solution in hexane, 1.85 mmol) which resulted in immediate gas evolution and precipitation of an orange solid. After stirring for 4 h at room temperature the precipitate was isolated, washed three times with hexane and dried under high vacuum: 0.77 g (69%). Crystals for the X-ray structure determination were obtained by recrystallization from warm benzene; m.p. 343 °C. ^{1}H NMR (300 MHz, C_6D_6, 25 °C): δ = 9.17 (s, 4 H, NC*H*), 7.80 [d, ^4J(H,H) = 2.1 Hz, 4 H, H_{aryl}], 7.06 [d, ^4J(H,H) = 2.1 Hz, 4 H, H_{aryl}], 6.90 [d, ^3J(H,H) = 8.1 Hz, 4 H, H_{aryl}], 6.13 [t, ^3J(H,H) = 8.1 Hz, 4 H, H_{aryl}], 1.67 (s, 36 H, *t*Bu), 1.41 (s, 36 H, *t*Bu) ppm. ^{13}C NMR (300 MHz, C_6D_6, 25 °C): δ = 171.8, 170.1, 156.4, 142.9, 136.8, 132.7, 132.1, 117.8, 116.1, 35.9, 34.0, 31.2, 29.7 ppm. $C_{140}H_{180}N_{12}O_8Zn_4$ (2420.58): C 69.47, H 7.50; found: C 69.62, H 7.72.

General Procedure for Lactide Polymerization: A Schlenk flask was charged in a glovebox with a solution of *rac*-lactide (250 mg, 1.73 mmol) in 2.5 mL of the specified solvent. A solution of the initiator (0.017 mmol) in the same solvent (500 mg) was added rapidly. The mixture was immediately stirred with a magnetic stir bar at the desired temperature for five hours. The reaction was quenched with methanol (10 mL) containing a few drops of concentrated aqueous HCl, and the polymer was precipitated with excess methanol. The polymer was then dried under vacuum to constant weight. Molecular weight distributions have been measured

Table 3. Crystal data for PARA-[MgN(SiMe$_3$)$_2$·(thf)]$_2$, [PARA-Ca·(thf)$_2$]$_2$, PARA-[CaN(SiMe$_3$)$_2$·(thf)$_2$]$_2$ and [PYR-Zn]$_4$.

Compound	PARA-[MgN(SiMe$_3$)$_2$·(thf)]$_2$	[PARA-Ca·(thf)$_2$]$_2$	PARA-[CaN(SiMe$_3$)$_2$·(thf)$_2$]$_2$	[PYR-Zn]$_4$
Formula	$C_{56}H_{98}Mg_2N_4O_4Si_4\cdot(C_6H_6)_2$	$C_{88}H_{124}Ca_2N_4O_8\cdot(C_6H_6)_4$	$C_{64}H_{114}Ca_2N_4O_6Si_4\cdot(C_6H_6)$	$C_{140}H_{180}N_{12}O_8Zn_4\cdot(C_6H_6)_{12}$
MW	1208.58	1758.50	1306.23	3357.83
Size [mm^3]	0.2 × 0.2 × 0.1	0.1 × 0.1 × 0.1	0.5 × 0.4 × 0.3	0.5 × 0.2 × 0.2
Crystal system	monoclinic	monoclinic	orthorhombic	monoclinic
Space group	*C*2/*c*	$P2_1/c$	$Pca2_1$	*C*2/*c*
a [Å]	43.349(5)	13.7721(11)	18.5829(10)	38.021(5)
b [Å]	10.3258(11)	18.4509(14)	17.3548(9)	17.104(2)
c [Å]	16.6335(18)	20.3988(15)	26.4108(15)	35.059(4)
α	90	90	90	90
β	110.401(7)	95.727(5)	90	106.109(7)
γ	90	90	90	90
V [Å^3]	7300.3(14)	5157.6(7)	8517.6(8)	21904(5)
Z	4	2	4	4
ρ [gcm^{-3}]	1.100	1.132	1.019	1.018
μ(Mo-K_α) [mm^{-1}]	0.144	0.167	0.195	0.484
T [°C]	–70	–70	–70	–100
θ (max.)	24.0	24.2	24.3	26.1
Total reflections, unique	34661, 5679	13628, 7155	146368, 13654	93728, 21702
R_{int}	0.128	0.109	0.139	0.069
Obsd. reflections [$I > 2\sigma(I)$]	3350	2597	9159	14400
Parameters	382	580	813	1087
R_1	0.0626	0.0592	0.0828	0.0654
*wR*2	0.1842	0.1966	0.2274	0.1740
GOF	1.01	0.82	1.04	1.06
max./min. residual e$^-$ [eÅ^{-3}]	–0.38/0.28	–0.28/0.35	–0.31/0.50	–0.64/0.37
Flack parameter	–	–	0.13(6)	–

by GPC measurements of polymer dissolved in chloroform. ^{1}H NMR measurements have been performed in $CDCl_3$.

Crystal Structure Determinations: All data were collected on a Siemens SMART CCD diffractometer (Table 3). The structures have been solved by direct methods (SHELXS-97)[20] and were refined with SHELXL-97.[21] The geometry calculations and graphics have been performed with PLATON.[22] All crystals contain one or more benzene molecules in the lattice. In the crystals of PARA-$[MgN(SiMe_3)_2\cdot(thf)]_2$, and [PARA-Ca·$(thf)_2]_2$ the enclosed benzene molecules were ordered and could be refined. The crystals of PARA-$[CaN(SiMe_3)_2\cdot(thf)_2]_2$ and $[PYR\text{-}Zn]_4$ contained some ordered benzene molecules that have been refined and some disordered benzene molecules which were treated with the SQUEEZE procedure incorporated in the program PLATON.[22] Crystals of $[PYR\text{-}Zn]_4$ are extremely sensitive and decompose fast in paraffin oil. This is likely due to large amounts of incorporated solvent (7 relatively ordered and 2 disordered benzene molecules are found in the asymmetric unit).

CCDC-678735 {for PARA-$[CaN(SiMe_3)_2\cdot(thf)_2]_2$}, -678736 {for [PARA-Ca·$(thf)_2]_2$}, -678737 {for PARA-$[MgN(SiMe_3)_2\cdot(thf)]_2$}, and -678738 (for $[PYR\text{-}Zn]_4$) contain the supplementary crystallographic data. These data can be obtained free of charge from The Cambridge Crystallographic Data Centre via www.ccdc.cam.ac.uk/data_request/cif.

Acknowledgments

We acknowledge the Deutsche Forschungsgemeinschaft (DFG) for support of this project within the AM^2-net framework. Prof. Dr. R. Boese and D. Bläser (University Duisburg-Essen) are thanked for collection of X-ray diffraction data.

[1] a) S. Harder, F. Feil, K. Knoll, *Angew. Chem.* **2001**, *113*, 4391–4394; *Angew. Chem. Int. Ed.* **2001**, *40*, 4261–4264; b) M. R. Crimmin, I. J. Casely, M. S. Hill, *J. Am. Chem. Soc.* **2005**, *127*, 2042–2043; c) F. Buch, J. Brettar, S. Harder, *Angew. Chem.* **2006**, *118*, 2807–2811; *Angew. Chem. Int. Ed.* **2006**, *45*, 2741–2745; d) M. R. Crimmin, A. G. M. Barrett, M. S. Hill, P. A. Procopiou, *Org. Lett.* **2007**, *9*, 331–333; e) M. R. Crimmin, A. G. M. Barrett, M. S. Hill, P. B. Hitchcock, P. A. Procopiou, *Organometallics* **2007**, *26*, 2953–2956; f) S. Datta, P. W. Roesky, S. Blechert, *Organometallics* **2007**, *26*, 4392–4394; g) F. Buch, S. Harder, *Organometallics* **2007**, *26*, 5132–5135; h) J. Spielmann, S. Harder, *Eur. J. Inorg. Chem.* **2008**, early view; i) M. R. Crimmin, A. G. M. Barrett, M. S. Hill, P. B. Hitchcock, P. A. Procopiou, *Organometallics* **2008**, *27*, 497–499.

[2] a) M. H. Chisholm, N. W. Eilerts, J. C. Huffman, S. S. Iyer, M. Pacold, K. Phomphrai, *J. Am. Chem. Soc.* **2000**, *122*, 11845–11854; b) Z. Zhong, P. J. Dijkstra, C. Birg, M. Westerhausen, J. Feijen, *Macromolecules* **2001**, *34*, 3863–3868; c) B. M. Chamberlain, M. Cheng, D. R. Moore, T. M. Ovitt, E. B. Lobkovsky, G. W. Coates, *J. Am. Chem. Soc.* **2001**, *123*, 3229–3238; d) M. H. Chisholm, J. Gallucci, K. Phomphrai, *Inorg. Chem.* **2002**, *41*, 2785–2794; e) M. H. Chisholm, J. Gallucci, K. Phomphrai, *Chem. Commun.* **2003**, 48–49; f) Z. Zhong, S. Schneiderbauer, P. J. Dijkstra, M. Westerhausen, J. Feijen, *Polym. Bull.* **2003**, *51*, 175–182; g) M. H. Chisholm, J. Gallucci, K. Phomphrai, *Inorg. Chem.* **2004**, *43*, 6717–6725; h) A. P. Dove, V. C. Gibson, E. L. Marshall, A. J. P. White, D. J. Williams, *Dalton Trans.* **2004**, 570–578; i) J.-C. Wu, B.-H. Huang, M.-L. Hsueh, S.-L. Lai, C.-C. Lin, *Polymer* **2005**, *46*, 9784–9792; j) Y. Sarazin, R. H. Howard, D. L. Hughes, S. M. Humphrey, M. Bochmann, *Dalton Trans.* **2006**, 340–350; k) D. J. Darensbourg, W. Choi, C. P. Richers, *Macromolecules* **2007**, *40*, 3521–3523; l) H.-Y. Chen, H.-Y. Tang, C.-C. Lin, *Polymer* **2007**, *48*, 2257–2262.

[3] a) M. Sawamura, M. Sudoh, Y. Ito, *J. Am. Chem. Soc.* **1996**, *118*, 3309–3310; b) R. C. Mathews, D. K. Howell, W.-J. Peng, S. G. Train, W. D. Treleaven, G. G. Stanley, *Angew. Chem.* **2006**, *118*, 2807–2811; *Angew. Chem. Int. Ed. Engl.* **1996**, *35*, 2253–2256; c) P. Molenveld, S. Kapsabelis, J. F. J. Engbersen, D. N. Reinhoudt, *J. Am. Chem. Soc.* **1997**, *119*, 2948–2949; d) R. G. Konsler, J. Karl, E. N. Jacobsen, *J. Am. Chem. Soc.* **1998**, *120*, 10780–10781; e) P. Molenveld, J. F. J. Engbersen, D. N. Reinhoudt, *Chem. Soc. Rev.* **2000**, *29*, 75–86; f) E. N. Jacobsen, *Acc. Chem. Res.* **2000**, *33*, 421–431; g) B. M. Trost, T. Mino, *J. Am. Chem. Soc.* **2003**, *125*, 2410–2411; h) D. R. Moore, M. Cheng, E. B. Lobkovsky, G. W. Coates, *J. Am. Chem. Soc.* **2003**, *125*, 11911–11924; i) G. M. Sammis, H. Danjo, E. N. Jacobsen, *J. Am. Chem. Soc.* **2004**, *126*, 9928–9929; j) Z. Weng, S. Teo, Z.-P. Liu, T. S. A. Hor, *Organometallics* **2007**, *26*, 2950–2952; k) C. Li, L. Chen, M. Garland, *J. Am. Chem. Soc.* **2007**, *129*, 13327–13334; l) C. Mazet, E. N. Jacobsen, *Angew. Chem.* **2008**, *120*, 1786–1789; *Angew. Chem. Int. Ed.* **2008**, *47*, 1762–1765; m) N. Guo, C. L. Stern, T. J. Marks, *J. Am. Chem. Soc.* **2008**, *130*, 2246–2261.

[4] a) E. J. Vandenberg, *Pure Appl. Chem.* **1976**, *48*, 295–306; b) W. Braune, J. Okuda, *Angew. Chem.* **2003**, *115*, 67–71; *Angew. Chem. Int. Ed.* **2003**, *42*, 64–68; c) E. Schön, X. Zhang, Z. Zhou, M. H. Chisholm, P. Chen, *Inorg. Chem.* **2004**, *43*, 7278–7280; d) G. W. Coates, D. R. Moore, *Angew. Chem.* **2004**, *116*, 6784–6806; *Angew. Chem. Int. Ed.* **2004**, *43*, 6618–6639; e) B. Y. Lee, H. Y. Kwon, S. Y. Lee, S. J. Na, S. Han, H. Yun, H. Lee, Y.-W. Park, *J. Am. Chem. Soc.* **2005**, *127*, 3031–3037; f) M. F. Pilz, C. Limberg, B. B. Lazarov, K. C. Hultzsch, B. Ziemer, *Organometallics* **2007**, *26*, 3668–3676.

[5] For reviews, see: a) A. L. Gavrilova, B. Bosnich, *Chem. Rev.* **2004**, *104*, 349–384; b) E. K. van den Beuken, B. L. Feringa, *Tetrahedron* **1998**, *54*, 12985–13011; c) H. Steinhagen, G. Helmchen, *Angew. Chem.* **1996**, *108*, 2489–2492; *Angew. Chem. Int. Ed. Engl.* **1996**, *35*, 2339–2342; d) N. Sträter, W. N. Lipscomb, T. Klabunde, B. Krebs, *Angew. Chem.* **1996**, *108*, 2158–2191; *Angew. Chem. Int. Ed. Engl.* **1996**, *35*, 2024–2055; e) C. Belle, C. J.-L. Pierre, *Eur. J. Inorg. Chem.* **2003**, 4137–4146; f) O. E. Fenton, *Chem. Soc. Rev.* **1999**, *28*, 159–168.

[6] a) S. Yamada, *Coord. Chem. Rev.* **1999**, *190–192*, 537–555; b) J. F. Larrow, E. N. Jacobsen, *Top. Organomet. Chem.* **2004**, *6*, 123–152.

[7] M. A. Van Aelstyn, T. S. Keizer, D. L. Klopotek, S. Liu, M.-A. Munoz-Hernandez, P. Wei, D. A. Atwood, *Organometallics* **2000**, *19*, 1796–1801.

[8] Metal···metal distances based on simple geometrical calculations using a general M–O and M–N distance of 2.5 Å.

[9] G. A. Morris, H. Zhou, C. L. Stern, S. T. Nguyen, *Inorg. Chem.* **2001**, *40*, 3222–3227.

[10] W. Ostwald, *Lehrbuch der Allgemeinen Chemie*, Engelmann, Leipzig, Germany, **1896**, vol. 2, part 1.

[11] a) D. G. Blackmond, *Chem. Eur. J.* **2007**, *13*, 3290–3295; b) W. L. Noorduin, T. Izumi, A. Millemaggi, M. Leeman, H. Meekes, W. J. P. van Enckevort, R. M. Kellogg, B. Kaptein, E. Vlieg, D. G. Blackmond, *J. Am. Chem. Soc.* **2008**, *130*, 1158–1159.

[12] a) N. Yoshida, K. Ichikawa, M. Shiro, *J. Chem. Soc. Perkin Trans. 2* **2000**, 17–26; b) A. W. Kleij, M. Kuil, D. M. Tooke, A. L. Spek, J. N. H. Reek, *Inorg. Chem.* **2007**, *46*, 5829–5831.

[13] A. Shafir, D. Fiedler, J. Arnold, *J. Chem. Soc., Dalton Trans.* **2002**, 555–560.

[14] C. A. Hunter, *Chem. Soc. Rev.* **1994**, *23*, 101.

[15] A. Trösch, H. Vahrenkamp, *Z. Anorg. Allg. Chem.* **2004**, *630*, 2031–2034.

[16] Y. Xiao, Z. Wang, K. Ding, *Macromolecules* **2006**, *39*, 128–137.

[17] P. D. Knight, P. N. O'Shaughnessy, I. J. Munslow, B. S. Kimberley, P. Scott, *J. Organomet. Chem.* **2003**, *683*, 103–113.
[18] M. Westerhausen, *Inorg. Chem.* **1991**, *30*, 96–101.
[19] D. J. Darensbourg, M. W. Holtcamp, G. E. Struck, M. S. Zimmer, S. A. Niezgoda, P. Rainey, J. B. Robertson, J. D. Draper, J. H. Reibenspies, *J. Am. Chem. Soc.* **1999**, *121*, 107–116.
[20] G. M. Sheldrick, *SHELXS-97, Program for Crystal Structure Solution*, **1997**, University of Göttingen, Germany.
[21] G. M. Sheldrick, *SHELXL-97, Program for Crystal Structure Refinement*, **1997**, University of Göttingen, Germany.
[22] A. L. Spek, *PLATON, A Multipurpose Crystallographic Tool* **2000**, Utrecht University, Utrecht, The Netherlands.

Received: March 26, 2008
Published Online: July 7, 2008

